Journal of Organometallic Chemistry 896 (2019) 188–193

Contents lists available at ScienceDirect

Journal of Organometallic Chemistry

journal homepage: www.elsevier.com/locate/jorganchem

Room temperature fast synthesis four-membered red iridium(III) complexes containing Ir–S–P–S structures for OLEDs

Ning Su [1], Cheng-Zhen Shen [1], You-Xuan Zheng*

State Key Laboratory of Coordination Chemistry, Jiangsu Key Laboratory of Advanced Organic Materials, School of Chemistry and Chemical Engineering, Nanjing University, Nanjing, 210023, PR China

ARTICLE INFO

Article history:
Received 30 April 2019
Received in revised form
2 June 2019
Accepted 14 June 2019
Available online 15 June 2019

Keywords:
Organic light-emitting devices
Four-membered iridium(III) complex
Room temperature fast synthesis
Ir–S–P–S structure
Efficiency

ABSTRACT

One S atom contained ligand triethylamine salt of diphenylphosphinodithioic acid (dpss) was firstly developed for two four-membered red-emitting iridium(III) complexes with Ir–S–P–S structures, $(tfmpiq)_2Ir(dpss)$ and $(tfmpqz)_2Ir(dpss)$, in which 1-(4-(trifluoromethyl)phenyl)isoquinoline (tfmpiq) and 4-(4-(trifluoromethyl)phenyl)quinazoline (tfmpqz) were employed as the cyclometalated ligands, respectively. Owing to strong bonding ability of sulfur and iridium atom, two Ir(III) complexes were obtained rapidly and efficiently at room temperature in 5 min. The computational Gibbs free energy changes of the complexes formation reactions further indicate that they are exothermic and thermodynamically beneficial processes. They show similar PL emissions at 620 and 621 nm, respectively. Using the two complexes as dopants, both organic light-emitting devices (OLEDs) exhibit good properties with the maximum luminance of 16 400 cd/m^2 and the maximum external quantum efficiency of 19.38%.

1. Introduction

Among different types emitters of organic light-emitting devices (OLEDs), phosphorescent iridium(III) complexes are outstanding candidates due to their high efficiency and colorful emissions [1–5]. In recent years, red OLEDs have a rapid development [6–9]. However, when we focus on the reported red Ir(III) complexes, most of their molecular structures have five or six membered ring structures with acetylacetone (acac) or pyridinic acid (pic) or their derivatives as ancillary ligands [10–14], but there are only few reports about four membered ring ones [15,16]. Moreover, the Ir(III) complexes with four-membered ring structures have more vertical N–Ir–N and S–Ir–S angles in ancillary ligands, which will make the distance of iridium atom and ancillary ligand short, therefore, they have a good advantage to boost metal to ligand charge transfer (MLCT) effect leading to red-shifted emissions and potential EL performances [17–19].Therefore, it is necessary to develop four-membered Ir(III) complexes in red OLEDs.

Furthermore, as respect to most reported Ir(III) complexes, they always were successfully prepared under the condition of prolonged heating and refluxing, which greatly increased the production costs [20,21].It is crucial to exploit novel ancillary ligands, which could be used to synthesize Ir(III) complexes rapidly at room temperature to improve the synthesis efficiency.

According to our previous work [22–25], sulfur atom contained ancillary ligands have strong coordination ability with iridium atom, therefore, it is feasible to introduce S atom into ancillary ligand to obtain Ir(III) complexes efficiently and rapidly at room temperature. Take this into consideration, in this work, one novel S atom contained ancillary ligand (triethylamine salt of diphenylphosphinodithioic acid (dpss)) was firstly developed for two four-membered red Ir(III) complexes $(tfmpiq)_2Ir(dpss)$ and $(tfmpqz)_2Ir(dpss)$ with Ir–S–P–S structures, in which 1-(4-(trifluoromethyl)phenyl)isoquinoline (tfmpiq) and 4-(4-(trifluoromethyl)phenyl)quinazoline (tfmpqz) were selected as cyclometalated ligands, respectively. As expected, both Ir(III) complexes were synthesized rapidly at room temperature in 5 min due to easy coordination of S atom with iridium atom. Gibbs free energy changes of the complexes formation reactions further prove that they are exothermic and thermodynamically beneficial processes. Using the two complexes as dopants, both devices achieve good performances with the maximum luminance (L_{max}) of 16 400 cd/m^2 and the maximum external quantum efficiency (EQE_{max}) of 19.38%.

* Corresponding author.
E-mail address: yxzheng@nju.edu (Y.-X. Zheng).
[1] Represents Su and Shen contributed equally to this paper.

https://doi.org/10.1016/j.jorganchem.2019.06.017
0022-328X/

2. Experimental section

2.1. General synthesis of the ancillary ligands and Ir(III) complexes

The suspension of chlorodiphenyl phosphine (1.00 g, 4.53 mmol) and S_8 (3.48 g, 13.59 mmol) and triethylamine (1.37 g, 13.59 mmol) in toluene (50 mL) were refluxed for 12 h. Then the precipitate was formed and filtered to get the ancillary ligand (dpss) as dark brown solid, it is used directly without purification. Then the ancillary ligand (800 mg, 2.28 mmol) and the chloro-bridged dimer $[(tfmpiq)_2Ir(\mu\text{-}Cl)]_2$ or $[(tfmpqz)_2Ir(\mu\text{-}Cl)]_2$ (0.76 mmol, 0.33 eq) were stirred in 2-ethoxyethanol (15 mL) at room temperature for 5 min. The crude products were purified with a flash silica gel column and then sublimated under vacuum to give red crystals.

$(tfmpiq)_2Ir(dpss)$ (yield: 85%). ^1H NMR (400 MHz, $CDCl_3$) δ 9.78 (d, $J = 6.5$ Hz, 2H), 8.90 (d, $J = 7.7$ Hz, 2H), 8.25 (d, $J = 8.4$ Hz, 2H), 7.99–7.90 (m, 2H), 7.81–7.74 (m, 4H), 7.70–7.62 (m, 4H), 7.43 (dd, $J = 8.4, 6.4$ Hz, 2H), 7.34–7.26 (m, 6H), 7.12 (d, $J = 7.2$ Hz, 2H), 6.53 (s, 2H). ^{19}F NMR (376 MHz, $CDCl_3$) δ - 62.91 (s). HRMS (*m/z*): calcd for $C_{44}H_{28}F_6IrN_2PS_2$ $[M+H]^+$ 987.1043, found 987.1047.

$(tfmpqz)_2Ir(dpss)$ (yield: 88%). ^1H NMR (400 MHz, $CDCl_3$) δ 10.45 (s, 2H), 8.85 (d, $J = 8.5$ Hz, 2H), 8.43 (d, $J = 8.4$ Hz, 2H), 8.21 (d, $J = 8.3$ Hz, 2H), 8.01 (t, $J = 7.7$ Hz, 2H), 7.87 (t, $J = 7.8$ Hz, 2H), 7.67–7.55 (m, 4H), 7.44 (dd, $J = 8.4, 6.5$ Hz, 2H), 7.32–7.27 (m, 4H), 7.21 (d, $J = 7.2$ Hz, 2H), 6.67 (s, 2H). ^{19}F NMR (376 MHz, $CDCl_3$) δ - 63.21 (s). HRMS (*m/z*): calcd for $C_{42}H_{26}F_6IrN_4PS_2$ $[M+H]^+$ 989.0948, found 989.0944.

3. Results and discussion

3.1. Synthesis and characterization

As shown in Scheme 1, novel S atom contained ligand (triethylamine salt of diphenylphosphinodithioic acid (dpss)) was prepared by refluxing the mixture of chlorodiphenyl phosphine (1.00 g, 4.53 mmol) and S_8 (3.48 g, 13.59 mmol) and triethylamine (1.37 g, 13.59 mmol) in toluene (50 mL) for 12 h, which was used directly without further purification. Two complexes were obtained by stirring μ-chloro-bridged dimer $[(tfmpiq)_2Ir(\mu\text{-}Cl)]_2$ or $[(tfmpqz)_2Ir(\mu\text{-}Cl)]_2$ with the ancillary ligand (dpss) in 2-ethoxyethanol under room temperature in 5 min with good yields as 85% and 88% for $(tfmpiq)_2Ir(dpss)$ and $(tfmpqz)_2Ir(dpss)$, respectively. Furthermore, both complexes were confirmed with ^1H NMR, ^{19}F NMR (see ESI), high resolution mass spectrometer (HRMS) and X-ray crystallography. Gibbs free energy changes (ΔG) calculated by the density functional theory (DFT) calculations [26–28] are −79.6 and −97.7 kJ/mol for the formation of $(tfmpiq)_2Ir(dpss)$ and $(tfmpqz)_2Ir(dpss)$, respectively (Fig. 1).

3.2. X-ray crystallographic analysis and thermal stability

The single crystals of two Ir(III) complexes are displayed in Fig. 2, the crystal information and bond lengths/angles data are shown in Table S1 and Table S2 (SI), respectively. Each Ir(III) complex contains two C^N main ligands and one S^S ancillary ligand. The four-membered Ir–S–P–S structure results in bigger S–Ir–S bite angles (80.2° and 79.2°, respectively). The Ir–S bonds lengths (2.528(2) –2.545(2) Å) are much longer than the Ir–C bond lengths (1.992(2) - 2.064(8) Å) and the Ir–N bond lengths (2.047(2) to 2.068(7) Å), which are similar to the reported five or six membered ring Ir(III) complexes [29,30].

The thermogravimetric analysis (TGA) measurements (Fig. S1 (SI)) show that both Ir(III) complexes have high decomposition temperatures (T_d) of 381 and 352 °C for $(tfmpiq)_2Ir(dpss)$ and $(tfmpqz)_2Ir(dpss)$ complexes (with 5% loss of weight, Table 1), respectively, suggesting they have good thermal stabilities.

3.3. Photophysical property

The UV/vis properties of two Ir(III) complexes are displayed in Fig. 3. The Ir(III) complex $(tfmpqz)_2Ir(dpss)$ exhibits a red-shifted absorption bands than $(tfmpiq)_2Ir(dpss)$ ranging from 230 to 600 nm due to one more nitrogen atom in tfmpqz cyclometalated ligand. The absorptions under 380 nm are definitely ascribed to ligand-centered (LC) transitions. While the other absorptions (380–600 nm) are attributed to metal-to-ligand charge transfer (MLCT) transitions. Both Ir(III) complexes show almost same PL emissions at 620 and 621 nm, respectively, suggesting the alteration of main ligands has little effect on their PL emissions. However, $(tfmpqz)_2Ir(dpss)$ complex displays much higher phosphorescence quantum yields (Φ_{PL}) of 0.68 than that of $(tfmpiq)_2Ir(dpss)$ complex (0.35) due to the N atom effect. The phosphorescent lifetime (τ_p) of two Ir(III) complexes are 1.99 and 2.21 μs (Table 1), respectively. These research results prove that two complexes with Ir–S–P–S structures are potential in OLEDs.

3.4. Electrochemical property and theoretical calculation

The highest occupied molecular orbital (HOMO) and the lowest unoccupied molecular orbital (LUMO) energy levels (E_{HOMO}/E_{LUMO}) of the Ir(III) complexes are significant for the OLEDs structures design. Cyclic voltammetry (CV) measurements were carried out to calculate these values of two complexes (Fig. S2 and Table 1). Obviously, $(tfmpqz)_2Ir(dpss)$ complex has lower E_{HOMO} (−5.75 eV) and E_{LUMO} (−3.50 eV) than that of $(tfmpiq)_2Ir(dpss)$ complex (−5.46 and −3.39 eV, respectively), which indicates that introducing one more N atom into cyclometalated ligand tfmpqz has great effect on their energy levels. The LUMO orbits of two complexes are largely distributed in π^* orbitals of C^N cyclometalated ligands (tfmpiq and

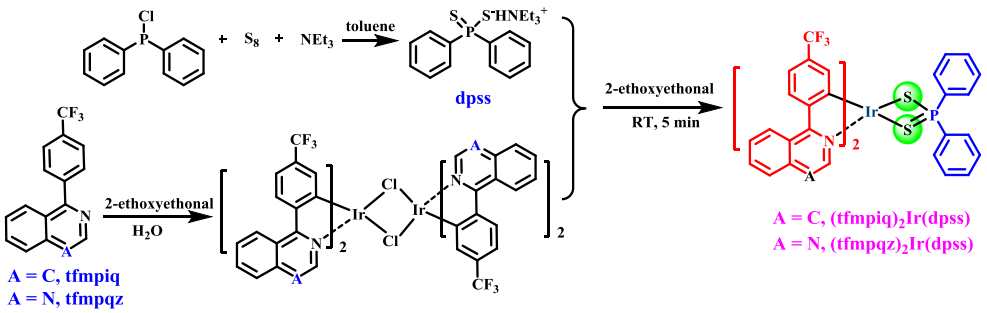

Scheme 1. Synthetic route of Ir(III) complexes.

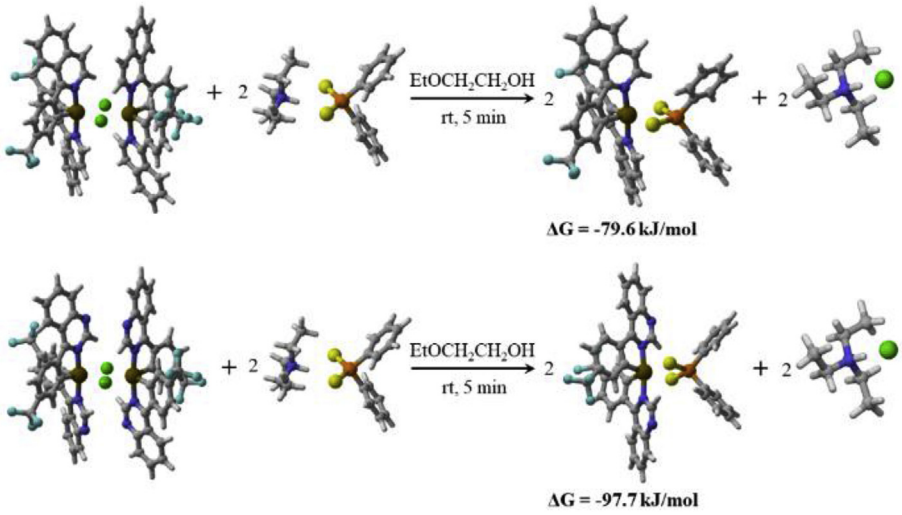

Fig. 1. The calculated Gibbs free energy change (ΔG) of the complexes formation reactions.

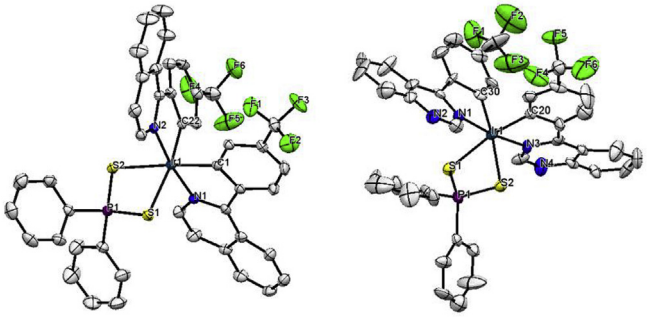

Fig. 2. ORTEP diagram of $(tfmpiq)_2Ir(dpss)$ (CCDC No. 1822170) and $(tfmpqz)_2Ir(dpss)$ (CCDC No. 1828577) with the atom-numbering schemes. Hydrogen atoms are omitted for clarity. Ellipsoids are drawn at the 50% probability level.

tfmpqz)(as high as 89.78% and 92.47%, respectively), while the HOMO orbitals mostly localize on π^* orbitals of C^N cyclometalated ligands (tfmpiq and tfmpqz) (47.45% and 44.45%, respectively) and the *d*- orbitals of iridium atom (47.68% and 48.95%, respectively), together with π orbitals of dpss ligand (4.77% and 6.60%, respectively) (Fig. S3 and Table S3).

3.5. Electroluminescent property

The devices with the structure of ITO/HATCN (hexaazatriphenylenehexacabonitrile, 5 nm)/TAPC ((*bis*(4-(*N*,*N*-ditolylamino)phenyl)cyclohexane, 40 nm)/TCTA (4,4′,4″-*tri*(9-carbazoyl) triphenyl amine, 10 nm)/$(tfmpiq)_2Ir(dpss)$ or $(tfmpqz)_2Ir(dpss)$: TCTA (4,4′,4″-*tri*(9-carbazoyl)triphenyl amine: TPBi (1,3,5-*tris*(1-phenyl-1*H*-benzimidazol-2-yl)benzene) (12 wt%, 10 nm)/TPBi (1,3,5-*tris*(1-phenyl-1*H*-benzimidazol-2-yl)benzene, 10 nm)/TmPyPB (1,3,5-*tri*((3-pyridyl)-phen- 3-yl)benzene, 40 nm)/LiF (1 nm)/Al (100 nm) were fabricated and named G1 and G2 to explore the electroluminescence (EL) performances of two complexes (Scheme 2), respectively. HATCN and TAPC are employed as hole-injecting and transport layer, respectively. LiF and TmPyPB are acted as electron-injecting and transport material, respectively. TCTA and TPBi are applied as host materials together. Moreover, TCTA and TPBi are selected as hole- and electron-blocking layer, respectively. Fig. 4 displays characteristics of devices G1 and G2 with the EL spectra, current efficiency (η_c) *versus* luminance, and power efficiency (η_p) *versus* luminance curves. The EL data are summarized in Table 2. Both devices have low turn-on voltage of 2.7 V (Table 2), which is owing to effective recombination of electrons and holes in the emitting layer (EML). The EL emissions of two devices are a little different from each other. Device G1 shows a emission peak at 612 nm and a shoulder peak at 654 nm, while device G2 exhibits a little red-shifted emission peak at 617 nm due to their individual main ligands. Two devices show red emissions with the Commission Internationale de 1′Eclairage (CIE) coordinates at (0.66, 0.34) and (0.65, 0.35), respectively.

Furthermore, due to the similar molecular structures of two complexes, their OLEDs performances are greatly related to their Φ_{PL}. For example, due to the lower Φ_{PL} of $(tfmpiq)_2Ir(dpss)$ ($\Phi_{PL} = 0.35$), device G1 exhibits a little lower device properties with a maximum luminance (L_{max}) of 6300 cd/m^2, a maximum current efficiency ($\eta_{c,max}$) of 8.22 cd/A, a maximum power efficiency ($\eta_{p,max}$) of 10.08 lm/W and a maximum external quantum efficiency

Table 1
Photophysical data of two iridium complexes.

Complex	T_d (°C)	PL[a] (nm)	Φ_{PL}[b] (%)	τ_p[c] (μs)	E_T (eV)[d]	E_{HOMO} (eV)[e]	E_{LUMO} (eV)[f]
$(tfmpiq)_2Ir(dpss)$	381	620	35	1.99	2.15	−5.46	−3.39
$(tfmpqz)_2Ir(dpss)$	352	621	68	2.21	2.10	−5.75	−3.50

[a] Measured in DCM (10^{-5} M) at room temperature.
[b] Measured in DCM (10^{-5} M) in N_2 atmosphere with a reference of *fac*-Ir(ppy)$_3$ ($\Phi_{PL} = 0.40$).
[c] Measured in DCM (10^{-5} M) in N_2 atmosphere.
[d] E_T (triplet energy): estimated from the highest-energy peaks of the 77 K phosphorescence spectra.
[e] Calculated from empirical equation: $E_{HOMO} = -(E_{ox} + 4.8)$ eV.
[f] Calculated from $E_{LUMO} = E_g^{opt} + E_{HOMO}$.

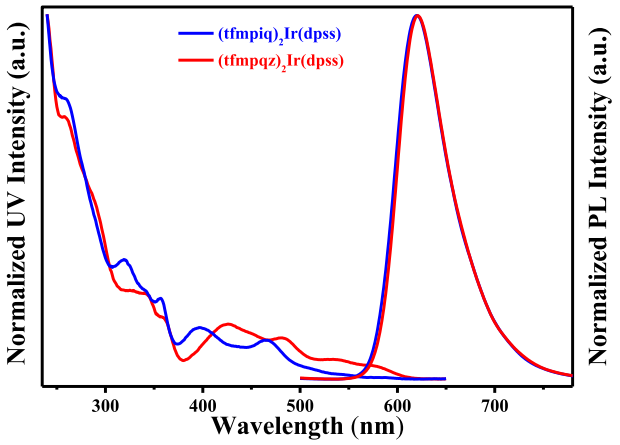

Fig. 3. Normalized absorption and emission spectra of the iridium complexes in dilute DCM (10^{-5} M) at room temperature.

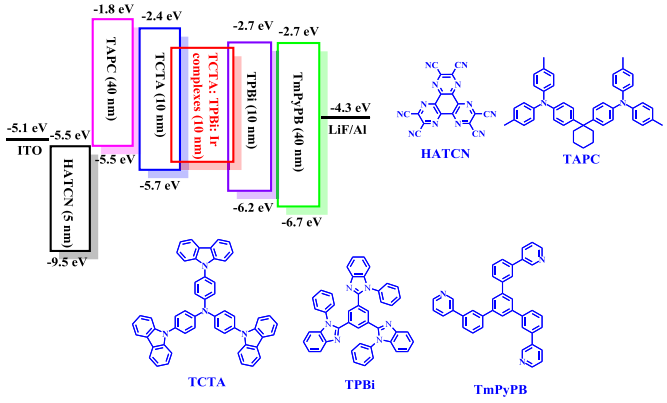

Scheme 2. The OLEDs device structure and their molecular structures used in this work.

(EQE$_{max}$) of 9.3%, respectively. The device G2 doping with (tfmpqz)$_2$Ir(dpss) complex ($\Phi_{PL} = 0.68$) shows better device performances with a L_{max} of 16 400 cd/m^2, a $\eta_{c,max}$ of 20.78 cd/A, a $\eta_{p,max}$ of 23.32 lm/W and an EQE$_{max}$ of 19.38%, respectively (Figs. S5 and SI).

In general, both devices doping with four-membered red Ir(III) complexes show good device performances, which is attributed to the following reasons. Firstly, novel S atom contained ancillary ligand dpss is successfully introduced into Ir(III) complexes forming four-membered Ir–S–P–S structures with large spatial steric hindrance, which can help supress molecular packing and TTA effect. Secondly, the reasonable OLEDs structures are designed, and the energy levels of Ir(III) complexes are follow in that of two host materials TCTA and TPBi, thus the energy transfer from the host to Ir(III) complexes are efficient in EML. Moreover, TCTA and TPBi are used as hole and electron blocking layer, respectively, which is beneficial for reducing the energy barrier between layers and further debase turn-on voltage. Lastly, nitrogen heterocycle in cyclometalated ligand would help improve the electron mobility of Ir(III) complex [31]. Therefore electrons and holes can be efficiently recombined in EML, which would improve OLEDs performances.

4. Conclusion

In summary, two four-membered red Ir(III) complexes (tfmpiq)$_2$Ir(dpss) and (tfmpqz)$_2$Ir(dpss) using S atom contained ligand with Ir–S–P–S structures were obtained rapidly at room temperature in 5 min. The much high negative calculated Gibbs free energy changes results (−79.6 and −97.7 kJ/mol) of the complexes formation reactions suggest that both reactions are exothermic and thermodynamically favorable processes. Employing the two red Ir(III) complexes, both devices achieve good OLEDs performances with the maximum luminance of 16 400 cd/m^2 and the maximum external quantum efficiency of 19.38%.

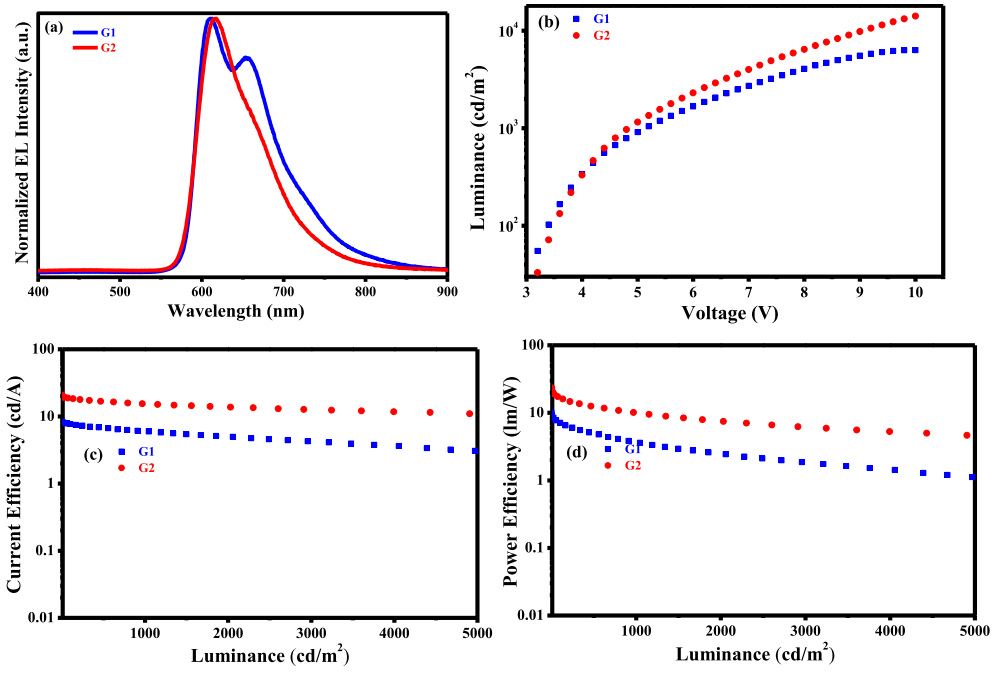

Fig. 4. Characteristics of devices G1 and G2: (a) EL spectra; (b) *L*-V curves; (c) η_c-*L* curves; (d) η_p-*L* curves.

Table 2
Key EL data of devices G1 and G2.

Device	V_{on} (V)[a]	L_{max} (cd/m^2)[b]	$\eta_{c,max}$ (cd/A)[c]	$\eta_{p,max}$ (lm/W)[d]	EQE_{max} (%)[e]	CIE (x,y)
G1	2.7	6300	8.22	10.08	9.30	(0.66,0.34)
G2	2.7	16 400	20.78	23.32	19.38	(0.65,0.35)

[a] Turn-on voltage, the driving voltage at 1 cd/m^2.
[b] Maximum luminance.
[c] Current efficiency.
[d] Power efficiency.
[e] External quantum efficiency calculated within visible spectrum region.

Acknowledgments

This work was supported by the National Natural Science Foundation of China (51773088).

Appendix A. Supplementary data

Supplementary data to this article can be found online at https://doi.org/10.1016/j.jorganchem.2019.06.017.

References

[1] X. Li, J. Zhang, Z. Zhao, L. Wang, H. Yang, Q. Chang, N. Jiang, Z. Liu, Z. Bian, W. Liu, Z. Lu, C. Huang, Deep blue phosphorescent organic light-emitting diodes with CIE *y* value of 0.11 and external quantum efficiency up to 22.5, Adv. Mater. 30 (2018) 1705005.
[2] A.K. Pal, S. Krotkus, M. Fontani, C.F.R. Mackenzie, D.B. Cordes, A.M.Z. Slawin, I.D.W. Samuel, E. Zysman-Colman, High-efficiency deep-blue-emitting organic light-emitting diodes based on iridium(III) carbene complexes, Adv. Mater. 30 (2018) 1804231.
[3] S. Lee, S.O. Kim, H. Shin, H.J. Yun, K. Yang, S.K. Kwon, J.J. Kim, Y.H. Kim, Deep-blue phosphorescence from perfluoro carbonyl-substituted iridium complexes, J. Am. Chem. Soc. 135 (2013) 14321–14328.
[4] C.H. Yang, Y.M. Cheng, Y. Chi, C.J. Hsu, F.C. Fang, K.T. Wong, P.T. Chou, C.H. Chang, M.H. Tsai, C.C. Wu, Blue-emitting heteroleptic iridium(III) complexes suitable for high-efficiency phosphorescent OLEDs, Angew. Chem. 46 (2007) 2418–2421.
[5] Y.C. Zhu, L. Zhou, H.Y. Li, Q.L. Xu, M.Y. Teng, Y.X. Zheng, J.L. Zuo, H.J. Zhang, X.Z. You, Highly efficient green and blue-green phosphorescent OLEDs based on iridium complexes with the tetraphenylimidodiphosphinate ligand, Adv. Mater. 23 (2011) 4041–4046.
[6] Z. Yan, Y. Wang, J. Ding, Y. Wang, L. Wang, Highly efficient phosphorescent furo[3,2-c]pyridine based iridium complexes with tunable emission colors over the whole visible range, ACS Appl. Mater. Interfaces 10 (2018) 1888–1896.
[7] P.N. Lai, C.H. Brysacz, M.K. Alam, N.A. Ayoub, T.G. Gray, J. Bao, T.S. Teets, Highly efficient red-emitting bis-cyclometalated iridium complexes, J. Am. Chem. Soc. 140 (2018) 10198–101207.
[8] F. Zhang, C. Si, X. Dong, D. Wei, X. Yang, K. Guo, B. Wei, Z. Li, C. Zhang, S. Li, B. Zhai, G. Cao, Iridium(iii) complexes bearing oxadiazol-substituted amide ligands: color tuning and application in highly efficient phosphorescent organic light-emitting diodes, J. Mater. Chem. C 5 (2017) 9146–9156.
[9] (a) P. Tao, Y. Miao, Y. Zhang, K. Wang, H. Li, L. Li, X. Li, T. Yang, Q. Zhao, H. Wang, S. Liu, X. Zhou, B. Xu, W. Huang, Highly efficient thienylquinoline-based phosphorescent iridium(III) complexes for red and white organic light-emitting diodes, Org. Electron. 45 (2017) 293–301;
(b) C.L. Ho, H. Li, W.Y. Wong, Red to near-infrared organometallic phosphorescent dyes for OLED applications, J. Organomet. Chem. 751 (2014) 261–285;
(c) Y. Zhang, Y. Wang, J. Song, J. Qu, B. Li, W. Zhu, W.Y. Wong, Near-infrared emitting materials via harvesting triplet excitons: molecular design, properties, and application in organic light emitting diodes, Adv. Opt. Mater. 6 (2018) 1800466;
(d) X. Yang, H. Guo, B. Liu, J. Zhao, G. Zhou, Z. Wu, W.Y. Wong, Diarylboron-based asymmetric red-emitting Ir(III) complex for solution-processed phosphorescent organic light-emitting diode with external quantum effciency above 28%, Adv. Sci. 5 (2018) 1701067;
(e) X. Liu, B. Yao, Z. Zhang, X. Zhao, B. Zhang, W.Y. Wong, Y. Cheng, Z. Xie, Power-efficient solution-processed red organic light-emitting diodes based on an exciplex host and a novel phosphorescent iridium complex, J. Mater. Chem. C 4 (2016) 5787–5794;
(f) X. Yang, G. Zhou, W.Y. Wong, Functionalization of phosphorescent emitters and their host materials by main-group elements for phosphorescent organic light-emitting devices, Chem. Soc. Rev. 44 (2015) 8484–8575.
[10] Z.W. Liu, M. Guan, Z.Q. Bian, D.B. Nie, Z.L. Gong, Z.B. Li, C.H. Huang, Red phosphorescent iridium complex containing carbazole-functionalized β-diketonate for highly efficient nondoped organic light-emitting diodes, Adv. Funct. Mater. 16 (2006) 1441–1448.
[11] C.L. Ho, W.Y. Wong, Z.Q. Gao, C.H. Chen, K.W. Cheah, B. Yao, Z.Y. Xie, Q. Wang, D.G. Ma, L.X. Wang, X.M. Yu, H.S. Kwok, Z.Y. Lin, Red-light-emitting iridium complexes with hole-transporting 9-arylcarbazole moieties for electro-phosphorescence efficiency/color purity trade-off optimization, Adv. Funct. Mater. 18 (2008) 319–331.
[12] D.H. Kim, N.S. Cho, H.Y. Oh, J.H. Yang, W.S. Jeon, J.S. Park, M.C. Suh, J.H. Kwon, Highly efficient red phosphorescent dopants in organic light-emitting devices, Adv. Mater. 23 (2011) 2721–2726.
[13] J. Kim, K.H. Lee, S.J. Lee, H.W. Lee, Y.K. Kim, Y.S. Kim, S.S. Yoon, Red phosphorescent bis-cyclometalated iridium complexes with fluorine-, phenyl-, and fluorophenyl-substituted 2-arylquinoline ligands, Chem 22 (2016) 4036–4045.
[14] P. Tao, W.L. Li, J. Zhang, S. Guo, Q. Zhao, H. Wang, B. Wei, S.J. Liu, X.H. Zhou, Q. Yu, B.S. Xu, W. Huang, Facile synthesis of highly efficient lepidine-based phosphorescent iridium(III) complexes for yellow and white organic light-emitting diodes, Adv. Funct. Mater. 26 (2016) 881–894.
[15] G. Li, D. Zhu, T. Peng, Y. Liu, Y. Wang, M.R. Bryce, Very high efficiency orange-red light-emitting devices with low roll-off at high luminance based on an ideal host-guest system consisting of two novel phosphorescent iridium complexes with bipolar transport, Adv. Funct. Mater. 24 (2014) 7420–7426.
[16] G. Li, P. Li, X. Zhuang, K. Ye, Y. Liu, Y. Wang, Rational design and characterization of heteroleptic phosphorescent complexes for highly efficient deep-red organic light-emitting devices, ACS Appl. Mater. Interfaces 9 (2017) 11749–11758.
[17] L. Chen, H. You, C. Yang, D. Ma, J. Qin, Novel, highly efficient blue-emitting heteroleptic iridium(III) complexes based on fluorinated 1,3,4-oxadiazole: tuning to blue by dithiolate ancillary ligands, Chem. Commun. 13 (2007) 1352–1354.
[18] Y. Liu, K. Ye, Y. Fan, W. Song, Y. Wang, Z. Hou, Amidinate-ligated iridium(III) bis(2-pyridyl)phenyl complex as an excellent phosphorescent material for electroluminescence devices, Chem. Commun. 25 (2009) 3699–3701.
[19] T. Peng, G. Li, K. Ye, C. Wang, S. Zhao, Y. Liu, Z. Hou, Y. Wang, Highly efficient phosphorescent OLEDs with host-independent and concentration-insensitive properties based on a bipolar iridium complex, J. Mater. Chem. C 1 (2013) 2920.
[20] H.Y. Li, L. Zhou, M.Y. Teng, Q.L. Xu, C. Lin, Y.X. Zheng, J.L. Zuo, H.J. Zhang, X.Z. You, Highly efficient green phosphorescent OLEDs based on a novel iridium complex, J. Mater. Chem. C 1 (2013) 560–565.
[21] Q.L. Xu, C.C. Wang, T.Y. Li, M.Y. Teng, S. Zhang, Y.M. Jing, X. Yang, W.N. Li, C. Lin, Y.X. Zheng, J.L. Zuo, X.Z. You, Syntheses, photoluminescence, and electroluminescence of a series of iridium complexes with trifluoromethyl-substituted 2-phenylpyridine as the main ligands and tetraphenylimidodiphosphinate as the ancillary ligand, Inorg. Chem. 52 (2013) 4916–4925.
[22] G.Z. Lu, N. Su, H.Q. Yang, Q. Zhu, W.W. Zhang, Y.X. Zheng, L. Zhou, J.L. Zuo, Z.X. Chen, H.J. Zhang, Rapid room temperature synthesis of red iridium(III) complexes containing four-membered Ir-S-C-S chelating ring for highly efficient OLEDs with EQE over 30%, Chem. Sci. 10 (2019) 3535–3542.
[23] X. Liang, F. Zhang, Z.P. Yan, Z.G. Wu, Y. Zheng, G. Cheng, Y. Wang, J.L. Zuo, Y. Pan, C.M. Che, Fast synthesis of iridium(III) complexes incorporating a bis(diphenylphorothioyl)amide ligand for efficient pure green OLEDs, ACS Appl. Mater. Interfaces 11 (2019) 7184–7191.
[24] J.C. Xia, X. Liang, Z.P. Yan, Z.G. Wu, Y. Zhao, Y.X. Zheng, W.W. Zhang, Iridium(III) phosphors with bis(diphenylphorothioyl)-amide ligand for efficient green and sky-blue OLEDs with EQE of nearly 28%, J. Mater. Chem. C 6 (2018) 9010–9016.
[25] X.F. Ma, J.C. Xia, Z.P. Yan, X.F. Luo, Z.G. Wu, Y.X. Zheng, W.W. Zhang, Highly efficient green and red electroluminescence with an extremely low efficiency roll-off based on iridium(III) complexes containing a bis(diphenylphorothioyl) amide ancillary ligand, J. Mater. Chem. C 7 (2019) 2570–2576.
[26] A.V. Marenich, C.J. Cramer, D.G. Truhlar, Universal solvation model based on solute electron density and on a continuum model of the solvent defined by the bulk dielectric constant and atomic surface Tensions, J. Phys. Chem. B 113 (2009) 6378–6396.
[27] P.J. Hay, W.R. Wadt, Ab initio effective core potentials for molecular calculations. Potentials for the transition metal atoms Sc to Hg, J. Chem. Phys. 82 (1985) 270–283.
[28] A.D. Becke, Density-functional thermochemistry. III. the role of exact exchange, J. Chem. Phys. 98 (1993) 5648–5652.
[29] E. Orselli, G.S. Kottas, A.E. Konradsson, P. Coppo, R. Frohlich, L. de Cola, A. van

Dijken, M. Buchel, H. Borner, Blue-emitting iridium complexes with substituted 1,2,4-triazole ligands: synthesis, photophysics, and devices, Inorg. Chem. 46 (2007) 11082–11093.

[30] Z.J. Xu, R. Fang, C. Zhao, J.S. Huang, G.Y. Li, N. Zhu, C.M. Che, Cis-Beta-bis(-carbonyl) ruthenium-salen complexes: X-ray crystal structures and remarkable catalytic properties toward asymmetric intramolecular alkene cyclopropanation, J. Am. Chem. Soc. 131 (2009) 4405–4417.

[31] (a) Y.Y. Liu, C.L. Song, W.J. Zeng, K.G. Zhou, Z.F. Shi, C.B. Ma, F. Yang, H.L. Zhang, X. Gong, High and balanced hole and electron mobilities from ambipolar thin-film transistors based on nitrogen-containing oligoacences, J. Am. Chem. Soc. 132 (2010) 16349–16351;
(b) T. Liu, M. Dupuis, C. Li, Band structure engineering: insights from defects, band gap, and electron mobility, from study of magnesium tantalite, J. Phys. Chem. C 120 (2016) 6930–6937.